Chemical Engineering Journal Advances 10 (2022) 100246

Contents lists available at ScienceDirect

Chemical Engineering Journal Advances

journal homepage: www.sciencedirect.com/journal/chemical-engineering-journal-advances

Electrochemical evaluation of different polymer binders for the production of carbon-modified stainless-steel electrodes for sustainable power generation using a soil microbial fuel cell

Imologie M Simeon [*,a,b], Katharina Herkendell [c], Deepak Pant [d], Ruth Freitag [a]

[a] Process Biotechnology, Faculty of Engineering science, University of Bayreuth, Universitätsstraße 30 FAN-D, 2. Stock, 95447 Bayreuth
[b] Department of Agricultural and Bioresources Engineering, PMB 65, School of Infrastructure, Process Engineering and Technology, Federal University of Technology, Minna, Nigeria
[c] Chair of Energy Process Engineering University of Erlangen-Nuremberg Fuerther Straße 244f, D-90429 Nuremberg, Germany
[d] Separation and Conversion Technology, Flemish Institute for Technological Research (VITO), Boeretang 200, Mol, 2400, Belgium

ARTICLE INFO

Keywords:
Electrochemical
Sustainable performance
Soil
Microbial fuel cell
Polymer binder
Electrode
bioelectricity

ABSTRACT

In this study, four different polymeric binders - polytetrafluoroethylene (PTFE), two-component epoxy (epoxy), polyvinyl alcohol (PVA), and polyvinylidene fluoride (PVDF) - were used to fabricate a surface-modified stainless-steel electrode. The polymeric binders were used to bond highly conductive carbon-black to a stainless-steel support using a simple fabrication method. The performance of the electrodes in terms of sustainable power generation was tested in a soil microbial fuel cell (SMFC). PTFE showed the fastest and best initial response in no-load operation, reaching a voltage of 370 mV after 7 days, compared to epoxy, PVA, and PVDF, which had 163, 151.7, and -26.7 mV, respectively. Electrochemical measurements showed that epoxy and PVDF have similar redox potential when operated as anode and cathode in an SMFC. Electrochemical evaluation of the long-term performance of the binders showed that epoxy gave 2.2-, 3.4-, and 4.9-fold higher performance than PVDF, PTFE, and PVA, respectively, under intermittent polarization. Although PVDF did not perform well in open circuits, it produced the highest current density in continuous operation with external loads. The most sustained performance was obtained with epoxy. This study has shown that epoxy can be a suitable and eco-friendly substitute for other binders using a simple fabrication method to produce high-performance anodes and cathodes for sustainable bioelectricity generation with a SMFC.

1. Introduction

Microbial fuel cells (MFCs) have received overwhelming research attention as a potential component of sustainable alternative energy resources. However, their low energy production rate requires both materials and architecture optimization to improve performance. One of the essential material components of MFCs is the electrode (anode and cathode). The electrodes are solid surfaces where the redox reaction occurs in an MFC, resulting in the removal of pollutants from the environment and electricity generation. The most commonly used electrode material is carbon [1], which is available as compact graphite sheets, rods, granules; fibrous material (felt, cloth, paper, fibers, foam); and glassy carbon. The use of metal-based electrodes has recently gained research interest due to their better conductivity and mechanical properties than carbon fiber materials [2]. Stainless-steel (SS) has emerged as the choicest metal electrode due to its high resistance to corrosion in an aqueous environment, its excellent conductivity, and mechanical properties [3]. However, surface modification is usually required to improve the surface for biofilm adhesion and thus increase the power density [4]. The use of nanocarbon or carbon granules as a catalyst for surface modification of SS is most common. In SS surface modification, polymeric adhesives are used to mechanically bond the surface modifier to the SS base to form a composite electrode of SS, polymer, and carbon.

The most common polymer binder in the fabrication of metal-carbon composite electrodes is a polytetrafluoroethylene (PTFE) suspension or powder [5–8]. Although Nafion has a relative advantage because it is a proton-conducting polymer with hydrophilic ion clusters and a transition region that allows effective proton transfer to the catalyst [9], it is being substituted as a binder in the construction of electrodes because of

* Corresponding author.
E-mail address: s.imologie@futminna.edu.ng (I.M. Simeon).

https://doi.org/10.1016/j.ceja.2022.100246
Received 30 October 2021; Received in revised form 8 January 2022; Accepted 10 January 2022
Available online 11 January 2022

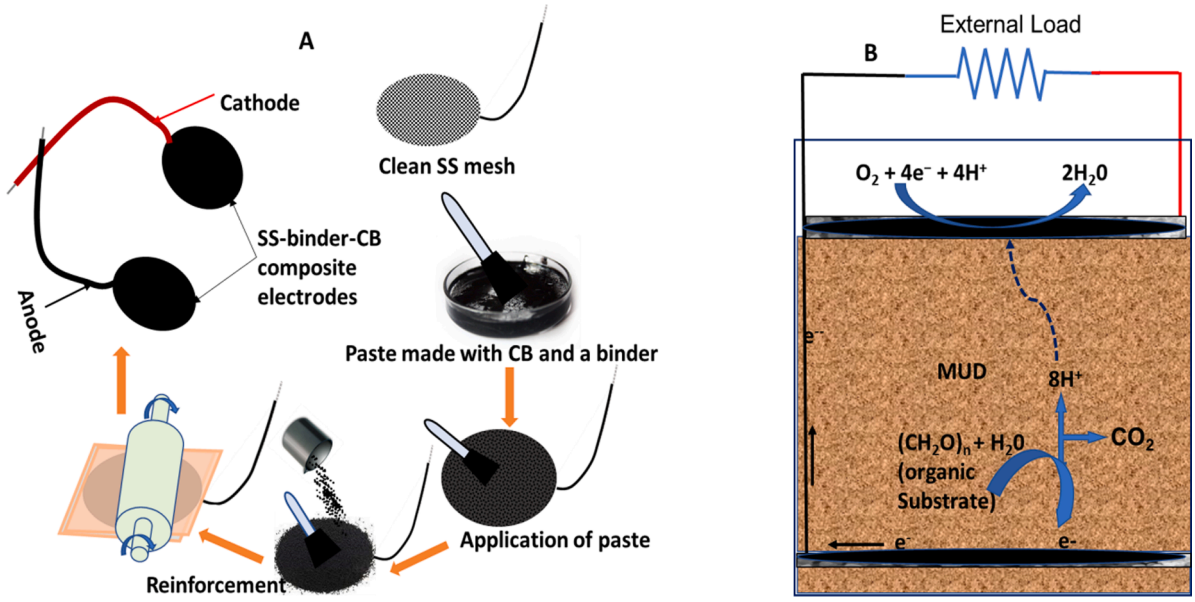

Fig. 1. A. Pasting and reinforcement process of electrode fabrication; B. Schematic and general principle of SMFC operation.

its high cost [5,10]. Electrodes made by bonding a mixture of PTFE and activated carbon (AC) to SS mesh are characterized by a simple fabrication process and a better performance/cost ratio (compared to Nafion and other conductive polymers) and long-term stability [11–13]). However, the use of PTFE in some reactor designs is limited due to its hydrophobic properties. This has the negative effect of drying out the catalyst environment, limiting effective proton transfer to the cathode [9]. Polyvinyl alcohol (PVA) has been proposed as an alternative to PTFE binder for anode electrocatalysts in MFCs due to its hydrophilicity (due to oxygen-containing groups) and biocompatibility [14,15]. Compared to the PTFE binder, the PVA binder was reported to provide about 98% higher power density in an *E. coli*-based MFC [14,16]. Due to the need to further reduce the production cost of composite electrodes, the possibility of replacing PTFE with either PVA or PlastiDip as a binder for a carbon-based cathode in an MFC was investigated [12]. The study found that although PTFE has the best electrochemical performance, PVA-based cathodes are promising alternatives that could be improved for higher power density. Recently, the use of a PVDF solution as a polymer binder for the fabrication of pseudocapacitive electrodes was reported [17]. Yang et al. [18] developed a MFC air cathode by a simple one-step phase inversion process using an SS base, a PVDF binder, and activated carbon. They reported that the air cathode fabricated with PVDF binder exhibited comparable power densities to cathodes made of more expensive binders such as PTFE. In a similar study, [19] tested a PVDF-based AC air cathode in serpentine up-flow MFCs operated continuously for more than six months using real domestic wastewater as substrate. The MFCs showed excellent and stable performance in household wastewater treatment and useful electricity generation. It was, therefore, suggested that PVDF/AC composite electrodes could be a cost-effective alternative for use in MFCs for wastewater treatment and useable power generation. Commercial two-component epoxy adhesives (epoxy) were also described as a suitable binder for surface modification of metal-based electrodes [16]. Epoxy resin as a binder is primarily based on its ease of fabrication, low cost, and better adhesive properties compared to other polymeric binders. The adhesive properties of epoxy make it the preferred binder for electrodes for solid-phase or Terrestrial MFCs for long-term bioelectricity generation [20,21].

Natural solid-phase MFCs are the most sustainable type because they have a perfect mix of microbiota and the natural starting substrate for the bio-electrochemical reactions in MFCs. Among natural solid-phase MFCs, the soil has received overwhelming research attention due to its diverse microbial population (c.a approximately 10^9 cells/g) and high organic content (approx. 100 mg/g) [22,23]. The soil thus provides inexhaustible electrons for the removal of environmental pollutants. However, the power density of soil microbial fuel cells SMFCs is still low because it is limited by the high internal resistance and the high oxygen cross-over to the anodic region [24]. Among other improvement strategies, surface-modified electrodes have been used in SMFCs [20]. However, optimization of the binder component of the composite electrode has not yet been studied for SMFCs. Among other properties, soil organic matter, nutrients, and heterogeneous soil microbial community affect the operation of SMFCs [25,26]. Although SMFCs are easy to assemble, however, as compared to water, the soil is much more complex due to its heterogeneous matrix and conditions. Therefore, the operation of SMFCs is more challenging than conventional MFCs due to these complicated operational mechanisms [27]. The choice of biocatalyst for electrode fabrication depends on the target substrate and process specifications [28]. In general, the metabolism of the electroactive microbes is the rate-limiting step, limiting current generation to the rate of substrate oxidation by the microbes [29]. However, the composition and surface chemistry of the electrode determines the efficiency of electron transfer from the substrate to the catalyst and between the catalyst and the electrodes and this inevitably affects the performance of the MFC [28]. Therefore, materials optimized for other MFCs (operated with purely cultured or systematically developed co-cultured *inocula*) may not perform as well in SMFCs due to their uniqueness.

A previous study [20], reported that electrodes made by using epoxy to bond carbon black to a SS base had better performance than a simple carbon felt electrode commonly used in SMFCs [3,30,31]. However, the performance of the electrodes was not optimized based on the binder component of the composites. In this study, the electrochemical performance of electrodes made of SS, carbon black (CB), and four different polymeric binders are compared. A simple fabrication process was used to bond a highly conductive CB to a SS wire mesh using PTFE, PVDF, EPOXY, or PVA as binders. Both the anode and cathode were fabricated using the same method and tested in a single-chamber soil-based MFC. Various electrochemical methods, including cyclic voltammetry (CV), linear sweep voltammetry (LSV), and electrochemical impedance spectroscopy, were used to compare the performance of the electrodes at ambient temperature. The effect of the binders on the long-term performance of the electrode under real-time external loading and no loading was investigated. Consequently, this study attempts to find the

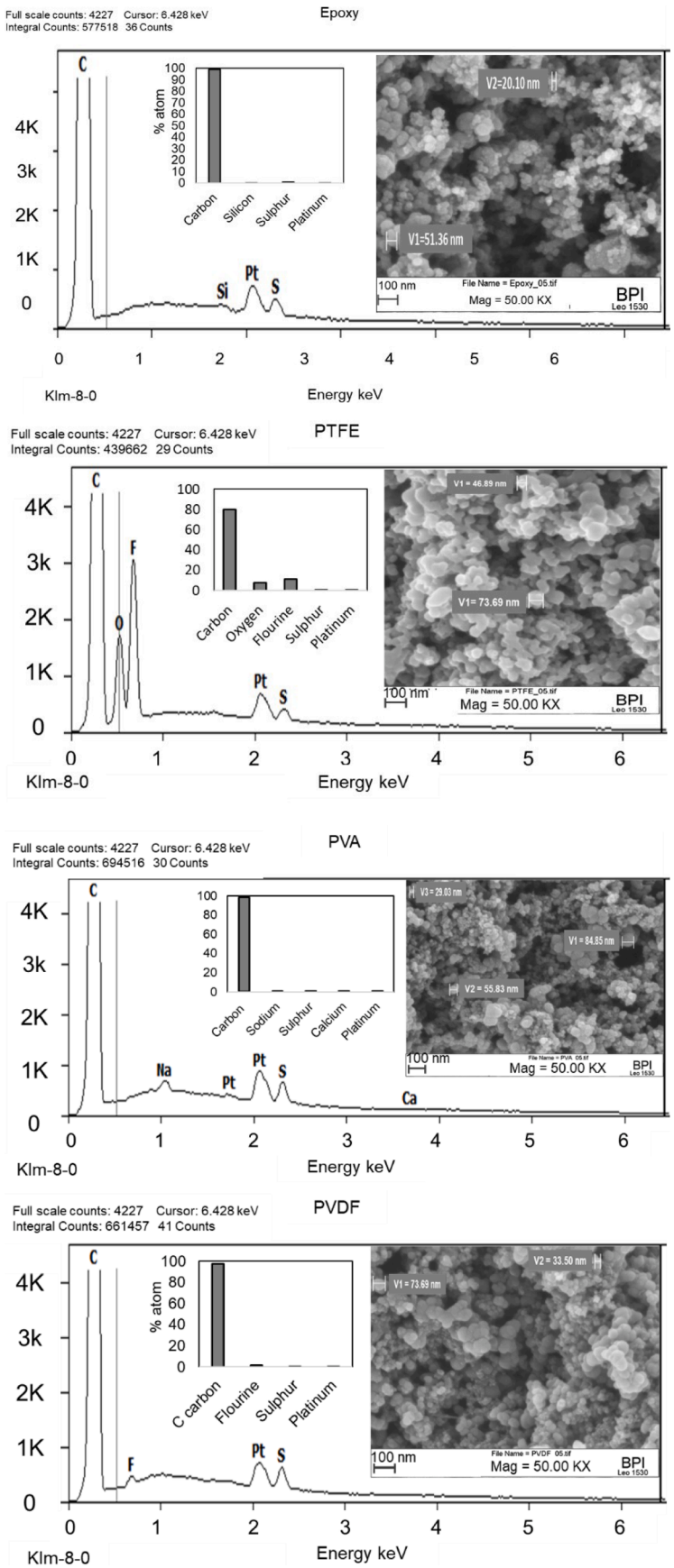

Fig. 2. EDX spectra showing surface compositions of the electrodes. (Insets: Left: Percentage atomic composition of the elements. Right: SEM images showing the bonding (cross-linking) of the CB atoms on the electrode and the particle sizes.).

best binder material for fabricating a SS surface-modified electrode to extract maximum sustainable bioelectricity from a soil-based single--chamber MFC in multiple batch operations.

2. Experimental

2.1. Electrodes fabrication

The binders used in the experiments are epoxy (UHU plus ENDfest, Germany), PTFE (60 wt% suspension in water), PVA (average weight Mw = 146,000 – 186,000; 87–89% hydrolyzed), PVDF (average weight, Mw = 534,000 by GPC powder). Apart from epoxy, all the other polymers were purchased from Sigma Aldrich. A simple fabrication process (referred to here as *pasting and reinforcement* (PR) was used (Fig. 1A). First, a mixture of CB (Cabot Vulcan XC-72, Quitech, Germany) was made into a viscous liquid (paste). The mixture was applied evenly to both surfaces of SS wire mesh (type 1.4301, Germany, with a mesh size of 0.315). After uniform application of the CB/binder mixture, reinforcement was performed by rapidly applying more CB on both sides of the electrode and pressing it between two flat metal surfaces (SS) several times. A ball-bearing rolling pin was used for manual pressing until cross-linking of the CB atoms on both sides occurred. This was done to reduce the electrode resistance and thus increase the conductivity for enhanced electron transfer [3]. The electrodes fabrication process was complete when a near-uniform surface was achieved and the electrode was electrically continuous between any two points and between the two sides of the electrodes. The continuity of the electrodes was checked with a professional multimeter (ET826). The electrodes were dried at room temperature (20.0 ± 1.5 °C) in a fume hood before use. Details of the amount of each binder and the CB used to make each electrode are given in Table S1. The CB used for producing the electrodes has a specific surface area between 18 and 550 m^2/g. For more information on the physical and chemical properties of Vulcan XC-72, please refer to Annex S1 of the supplementary document.

2.2. Electrode surface characterization

The microstructure, surface morphology, and chemical composition were characterized using a scanning electrode microscope (SEM) equipped with energy dispersive X-ray (EDX) spectroscopy. For the SEM/EDX study, approximately 1 cm^2 electrode prepared using each binder (as described in Section 2.1) was used for each composite electrode.

2.3. MFCs assembly and operation

The MFCs were constructed in a single chamber configuration (Fig. 1B) with biologically active sludge (pH = 7.32, conductivity = 2.25 mS/cm) from topsoil and garden compost [20,21]. Each MFC contained a mixture of equal amounts of topsoil and garden compost saturated with tap water to form the nutrient-rich medium, the source of electroactive bacteria, and the proton exchange membrane. A fixed anode-cathode distance of 4 cm was maintained, and approximately 1 cm of sludge was added to the bottom of each cell before anode installation [23]. The MFCs were left disconnected overnight, and excess water was drained from the cells the next day before connecting them to the data acquisition system (ADC-24). Data were collected every 1 hour throughout the operation (unless otherwise specified). Three MFCs were built for each binder (to form three groups A, B, and C) and operated in either open-circuit or closed-circuit with different external loads. To test the effect of the external load and the timing of the connection of the load, group A and group B were operated with a 1 kΩ resistor. The external load was connected to group A at the exponential growth rate of OCV (which also represents the logarithmic growth phase of the anodic biofilm), while the load was connected to group B from the beginning (lag phase) of the experiment. In contrast, the MFCs in group C were

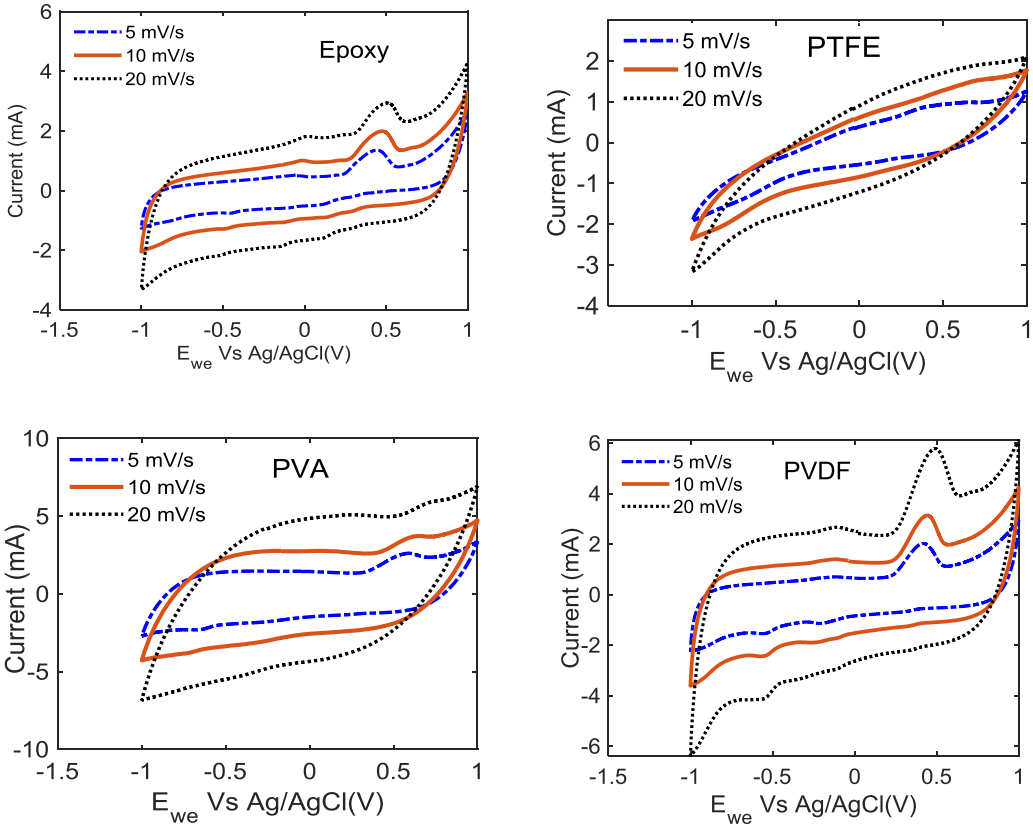

Fig. 3. Cyclic voltammetry of the binder performed in SUM.

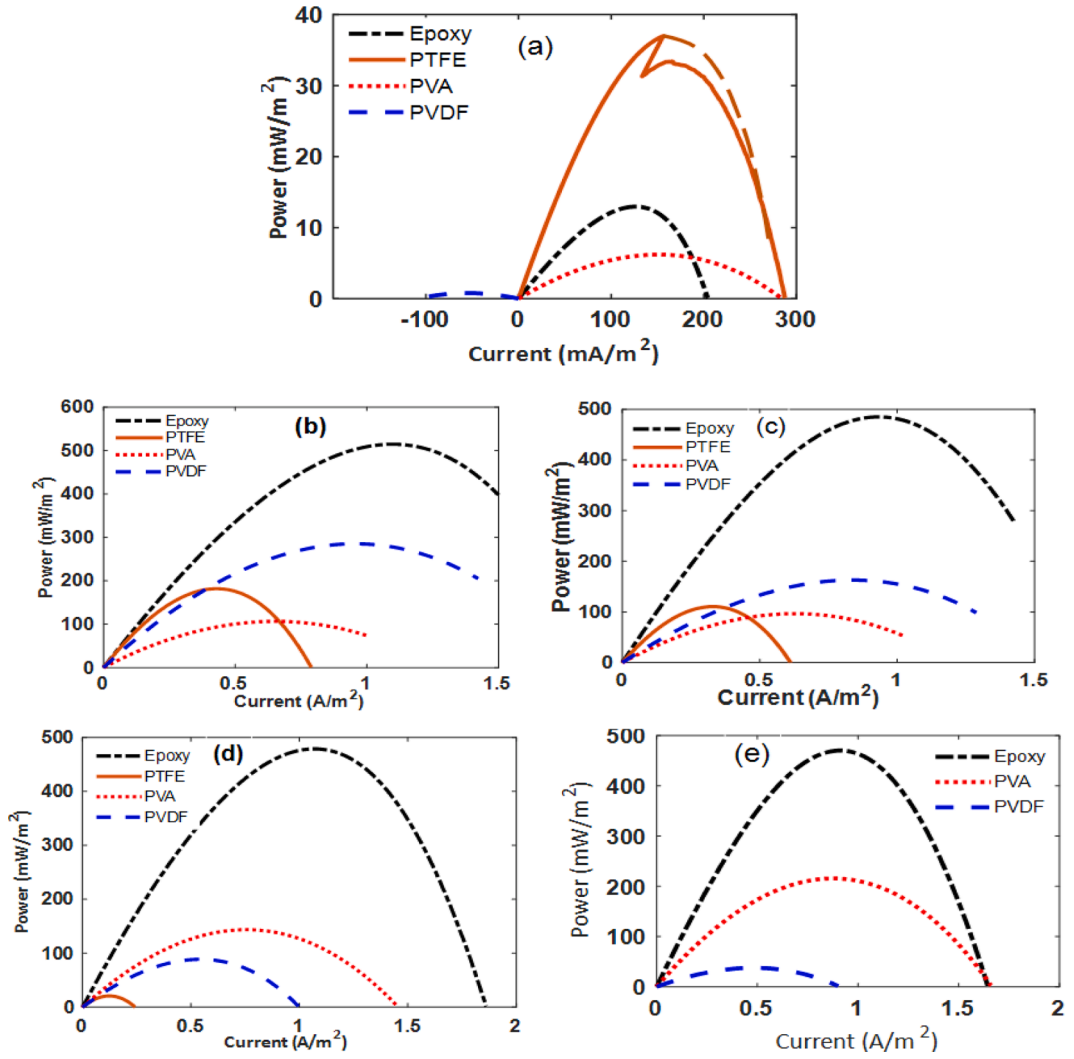

Fig. 4. performance curves (determined from two different groups) of the binder at different times during operation: (a) initial LSV with group A after 162 h of set-up; (b) and (c) performance determined from groups A and C after 30 days; (d) and (e) final performance determined from group B and C after 54 days. The distorted part of the PTFE curve in (a) was caused by a distortion of the connection point of the MFC to the potentiostat during the measurement. Therefore, the part indicated by the dashed line was used to determine the MPP parameters.

operated with 470 Ω resistors from the beginning. During the long-term stability test, the substrate was replenished with synthetic wastewater (SW) prepared as previously described [21] and the current density (j) delivered by the MFC through an external load (r) was calculated from

$$j = \frac{\mathrm{v}}{A_{an} r} \tag{1}$$

Where v is the voltage measured across r and A_{an} is the anode geometric surface area.

2.4. Electrochemical assessment

Three electrochemical methods were used to evaluate the performance of the MFCs using the VMP3 biological electrochemical workstation (France). Linear sweep voltammetry (LSV) was used to determine the potentiodynamic polarization curves or the electrochemical power characteristic (I-P) curves of the MFCs at different points. All LSV experiments were performed on a whole-cell basis with the circuit open and a potential scan rate (PSR) of 1 mV/s (unless otherwise stated). The maximum power density (P_d) delivered by the MFCs was calculated from the maximum power point (MPP) of the I-P characteristics curves according to Eq. (1)

$$P_d = \frac{V^2}{A_{an} R} = \frac{I^2 R}{A_{an}} \tag{2}$$

Where V and R are the voltage and resistance, respectively, at MPP.

Cyclic voltammetry (CV) was used to determine the redox potential of the electrodes in a fresh substrate [29], using PSR between 5 and 20 mV/s. Electrochemical impedance spectroscopy was performed in a two-electrode full-cell configuration (with the anode as the working electrode and the cathode as the reference and counter electrode). For the CV measurement, a single-chamber electrochemical cell was used with 50 mM phosphate buffer or SW as the working electrolyte, a piece of the anode (approximately 0.5 cm^2) served as the working electrode, the counter electrode was a platinum wire, and the reference electrode was Ag/AgCl electrode.

3. Results and discussion

3.1. Analysis of electrode surface morphology and chemical composition

Fig. 2 shows the SEM images and SEM/EDX spectra of the corresponding electrodes resulting from the PR fabrication process using the different polymer binders. The electrode surface consists of coarse and

Table 1
(a): Initial performance before external load was connected.

*(a): Initial performance before external load was connected				
Parameters	**Epoxy**	**PTFE**	**PVA**	**PVDF**
Eoc (mV)	163	370	151.7	−26.7
P_{max} (mW/m^2)	13	37	6.2	0.8
I (mA/m^2)	126.4	156.2	151.7	−55.8
V (mV)	102.6	236.9	40.9	−14
R (Ω	244.6	457.2	81.1	5.6
**(b): LSV measurement after 720 h (30 days) of operation				
Parameters	**EPOXY**	**PTFE**	**PVA**	**PVDF**
Eoc (mV)	802 ± 18	687 ± 73.0	305.5 ± 11.5	457.5 ± 106.5
Pmax (mW/m^2)	499.7 ± 14.8	146.2 + 35.6	101.3 ± 4.7	224.1 ± 61
I (A/m^2)	1.0 ± 0.1	0.4 ± 0.1	0.6 ± 0.1	0.9 ± 0.1
V (mV)	494.8 ± 22.4	381 ± 45.5	159.4 ± 6.2	248.1 ± 52.7
R (Ω	162.9 ± 32.6	366.6 ± 59.9	88.8 ± 11.2	89.3 ± 6.4
***(c): Final MPP parameters measured after 54 days				
Parameters	EPOXY	PTFE	PVA	PVDF
Eoc (mV)	787.5 ± 38.5	330	415.5 ± 50.5	220.5 ± 75.5
Pmax (mW/m^2)	474.6 ± 4.2	20.8	179.6 ± 36	63.1 ± 25.6
I (A/m^2)	1 ± 0.1	0.1	0.8 ± 0.1	0.5 ± 0.03
V (mV)	482.5 ± 36.2	171.7	216.4 ± 28.3	121.1 ± 42.6
R (Ω)	163.9 ± 38.5	426.4	86.3 ± 12	74.5 ± 16.5

* values were obtained from Fig. 4(a) **; Values are averages calculated from Fig. 4(b) and 4(c); *** values are averages obtained from Fig. 4(d) and 4(e). Subsequent LSVs (performed after 720 h (30 days) and 1620 h (54 days)) showed a drastic deterioration in the performance of PTFE. As shown in Fig. 4 and Table 2, epoxy showed better and more durable performance compared to the other binders. PVDF produced higher performance than PTFE and PVA in the second cycle of LSV tests, but towards the end, PVA showed better performance than PVDF and PTFE.

nano-porous carbon particles with sizes between 20 and 90 nm, systematically arranged and bonded with the binders. Due to the insulating properties of the polymer binders, the PR fabrication process was aimed at increasing the percentage composition of CB atoms on the electrodes to achieve higher conductivity for improved electron transfer. The surface carbon atom compositions were 98.9, 80.2, 98.7, and 97.5 for epoxy, PTFE, PVA, and PVDF, respectively. PTFE, which had the lowest carbon atom composition, had about 11.2% fluorine. PVDF also contained 1.6% fluorine. The presence of fluorine in PTFE and PVDF is obviously because the binders are fluorinated polymers. All the electrodes also had traces of other elements which were probably from impurities during preparation. The presence of platinum is due to the coating of the electrodes before SEM/EDX measurement.

3.2. Electrochemical performance of the binders

3.2.1. Cyclic voltammetry test

To study the redox potentials in terms of electron acceptance of the electrodes from the substrate, CV was performed in SW). Fig. 3 shows the CV voltammograms obtained with 3 PSRs at zero potentials Vs OCV. Visible oxidation peaks were obtained for epoxy, PVA, and PVDF within a wide potential window of −1 and 1 V against the Ag/AgCl reference electrode. The redox peaks were measured against the non-faradaic current baseline.

Using PSR of 5 mV/s as a reference, the peak oxidation current (Ipa) of epoxy, PVA and PVDF were 0.8095 mA (at 0.4384 V), 0.8203 (at 0.569 V), and 1.275 mA (at 0.4119 V), respectively. The CV showed irreversible electron transfer to the electrode due to oxidation of the substrate. The absence of corresponding reduction peaks in the voltammograms indicates the irreversibility of the redox process. Only PVDF and epoxy exhibit reduction peaks located at approximately the same potential position (in the negative direction) as the oxidation peaks, but the cathodic currents were negligible compared to the anodic peak currents. Chemical irreversibility concerning electrode materials indicates a lack of thermodynamic equilibrium at the electrode-solution interface, which may limit power output [32]. However, the electrodes in this study were not tested with standard electrolytes to determine the actual reaction kinetics. SW was chosen as the electrolyte for testing to investigate the behavior of the electrodes in wastewater environments where MFCs are commonly used. The CV results show that PVDF can produce higher currents compared to other electrodes, but epoxy also exhibits similar behavior to PVDF. The lack of clear peaks in the PTFE voltammograms could be due to the inadequacy of the PR method in fabricating the PTFE electrode. To ensure that the peaks observed here were due to oxidation of the substrate, background CVs were also performed using an inert electrolyte (50 mM phosphate buffer), and background currents due to the non-faradaic process during the experiment were compared to the CVs performed in SW. (see FigS1 of the supplementary documents).

3.2.2. Electrochemical power characteristics of the MFCs

The initial current-power (I-P) characteristics (determined by LSV) were performed with Group A at a potential scan rate of 0.1 mVs^{-1} after 162 h of open-circuit operation, during which all MFCs (except PVDF) produced OCV at an exponential rate (supplementary document). This initial performance evaluation was performed before each MFC in the group was connected to a 1 kΩ resistor. Subsequently, the power curves of groups A and C and B and C were determined after the external loads were disconnected and the MFCs were operated at no load. Fig. 4 shows the I-P characteristics of the MFCs.

From the initial I-P characteristics, PTFE shows an initial better performance than the other binders. The parameters of the MPP from Fig. 4 are shown in Table 1(a). Table 1b and 1c show the subsequent average performance obtained by two groups.

3.2.3. Electrochemical impedance spectroscopy

For all groups, the EIS was performed at two steady states - near the end of the lag phase and the maximum OCV in the steady state. Fig. 5 shows the Nyquist impedance and the corresponding Bode impedance plots of EIS performed at the steady OCV. From these plots, it can be deduced that the electrodes fabricated with epoxy and PVDF as binders have similar electrochemical properties. This is consistent with the cyclic voltammetry results shown in Fig. 3. Due to the obvious differences, the same electrical equivalent circuit could not be used to model the charge transfer kinetics and mass transfer properties of all the binders. The EIS parameters of epoxy, PVA, and PVDF were modeled using the equivalent electrical circuit $R1+Q_a/R_a+Q_c/(R_c+ W)$. Here, R1 is the ohmic resistance, Q_a and Q_c are constant phase elements used to model the anode and cathode double-layer capacitance connected in parallel to R_a and R_c which represent the anode and cathode charge transfer resistance. W is the Warburg impedance coefficient. PTFE on the other hand showed a one-step process without diffusion and was modeled with $R1+Q_a/R_a + Q_c/R_c$.

Table 2 presents the impedance parameters obtained by fitting simulated data of Fig. 5 to the experimental data using the equivalent circuits. Epoxy and PVDF had very similar ohmic resistance, but the charge transfer resistance of epoxy is about three times higher. Compared to epoxy, PVA and PVDF, PTFE had 21.6-, 18.06- and 66-times higher charge transfer resistance, respectively. PTFE showed negligible diffusional mass transfer but was limited by high charge transfer resistance. This is indicative of high concentrations of redox species leading to low currents [33]. The similarity in the electrochemical performance of Epoxy and PVDF could be due to their better adhesion to the SS current collector. For example, epoxy and PVDF were still firmly bonded to the SS support at the end of the experiment, while detachment was observed for PVA and PTFE. Since PVA showed a tendency to higher current at low voltage, a higher degree of hydrolysis (e.g. 97–99%) with better adhesiveness to hydrophobic materials [34] like CB would likely have resulted in better performance. Due to the

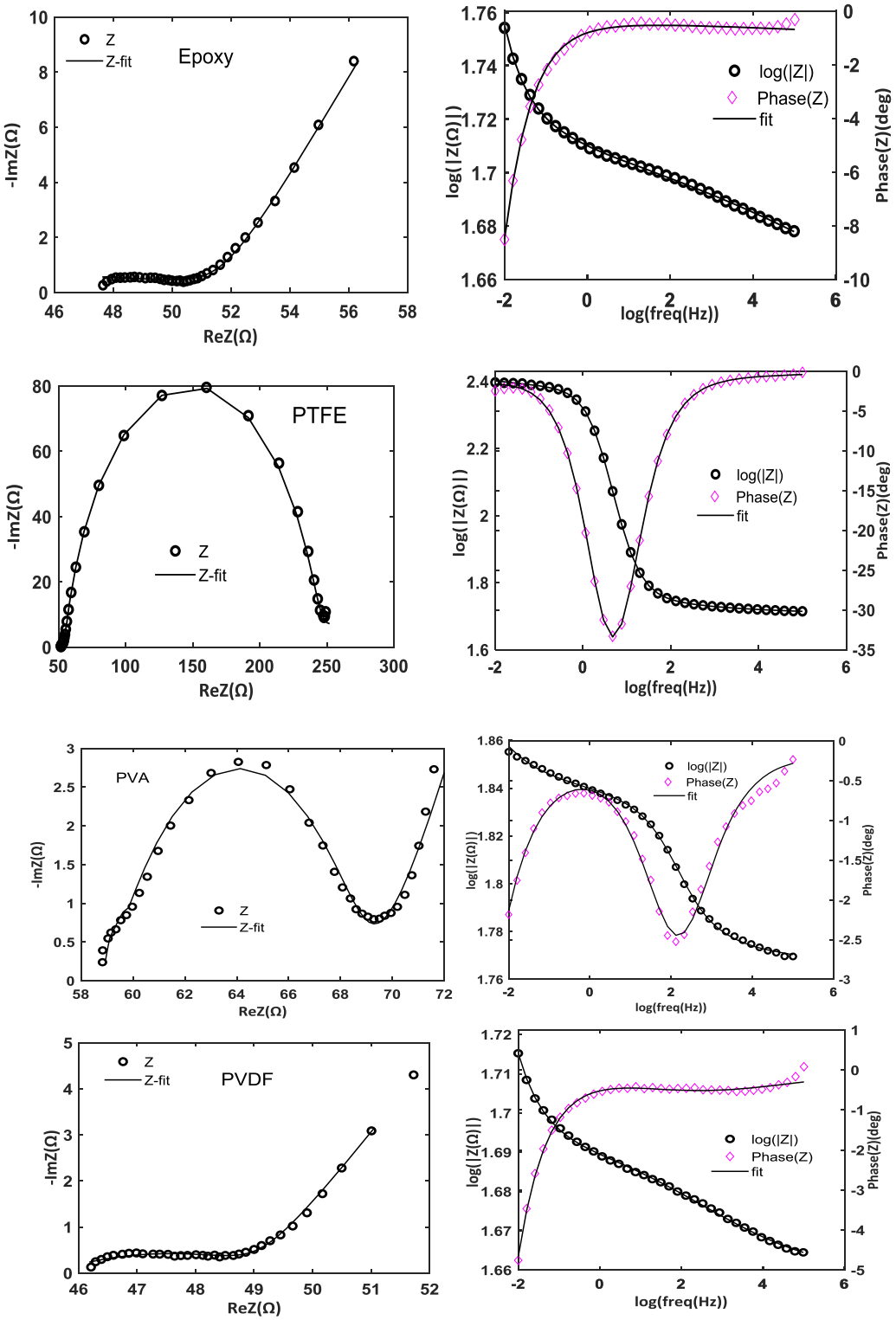

Fig. 5. Nyquist impedance (left); Bode impedance (right) of the MFCs measured at the steady OCV. The electrochemical characteristics obtained from Fig. 5 using the equivalent electrical circuit models are presented in Table 4.

deformation of PTFE and PVA, their charge transfer resistance at the end of the experiment increased compared to the initial values (FigS2 of the supplementary document).

In addition to the flaking of the PVA and PTFE electrodes, the larger charge transfer resistance compared to the initial values could also be due to the accumulation of organic material on the anode or a concentration of charge on the anode due to the slow reaction kinetics at the electrodes [9].

3.3. Performance of the binders at real-time external loads

To test the performance of the binders in continuous closed-circuit operation, the MFCs were tested with two real-time electronic loads (1 kΩ and 470 Ω), as described in the experimental section. Fig. 6 shows

Table 2
Fitted EIS parameters with the equivalent circuit.

Element	Epoxy	PTFE	PVA	PVDF
R_{Ohmic} (Ω)	46.24	51.7	58.5	45.91
C_{dl} (μF)	9.99	0.023	8.77	4.4
R_{ct} (Ω)	9.04	196.9	10.7	2.982
Q_c (F. s^(a-1))	0.377	2.3E-08	0.002	0.046
a	0.724	0.864	0.64	0.32
s	0.711		0.784	0.6068

R_{Ohmic} is the sum of all the Ohmic resistance, C_{dl} is the double layer capacitance calculated from Q_a, Q is a constant phase element denoted Qa and Qc for anode and cathode, respectively, in the equivalent circuit; a is the coefficient of Q, s is the Warburg impedance coefficient. R_{ct} was obtained by adding Ra (anodic charge transfer resistance) and Rc (cathodic charge transfer resistance) in the circuit since EIS was measured on a full-cell basis.

the continuous current generated by the MFCs. Fig. 6(a) and 6(b) show the performance of the MFCs in group A. A 1 kΩ resistor was connected to the MFCs when an exponential growth rate was observed under open-circuit (FigS3), as explained earlier. After the initial decrease in the current (indicating pseudo-capacitive behavior of the electrodes), a rapid increase in current was initially observed at PTFE, which reached a maximum current (j= 28.93 mA/m^2) after 49 h when the load was connected; thereafter, deterioration set in, as also observed in the LSV experiment. Epoxy showed a gradual current increase to a stable maximum current (j= 69.32 mA/m^2) after 236 h. PVDF showed a systematic current increase following the trend of a typical microbial growth cycle, which has the lag phase (1), exponential growth phase (2), stationary phase (3), death phase (4), another lag phase (5), and an exponential decay leading to current reversal (6). The maximum current produced by PVDF was 91.32 mA/m^2 after 169 h under the external load. It is worth noting that no voltage rise was obtained with PVDF before connecting the external loads. This indicates that the current generated after the connection of the external load is exclusively due to electron transfer as a result of the metabolic activities of the electroactive biofilm on the electrodes. The pronounced microbial growth phases also confirm this assertion. PVA, on the other hand, showed the slowest and lowest response to this external loading, reaching a maximum current of 14.47 mA/m^2 after 266 h. The maximum specific growth rates of the cells were estimated by fitting the experimental data to the modified Gompertz model according to Equation 3.

$$V = V_{max} \cdot \exp\left(-\exp\left(\frac{\mu_{max} \cdot e}{V_{max}} \cdot (\lambda - t) + 1 \right) \right) \quad (3)$$

where V_{max} is the maximum voltage reached with the external load, λ is the delay time, and e (2.71828) is Euler's constant. The estimated μ_{max} per hour for epoxy, PTFE, PVA, and PVDF with a 1 kΩ resistor are 0.0015, 0.0013, 0.0002, and 0.0033 respectively. The results show that bacterial growth with the binder was a limiting factor for bioelectricity production [35].

We hypothesized that starvation due to substrate depletion contributed to the rapid decline observed with PTFE and PVDF (Fig. 6(a)). The substrate was initially not replenished (apart from the occasional injection of water to replenish moisture that may have been lost from the system due to evaporation) to investigate the binder performance under starvation conditions and the recovery rate of cells after a period of starvation. After 317 h (about 13 days) of operation, the external load was disconnected from each cell, and the MFCs were treated with SW to replenish the substrate for microbial metabolism. The MFCs were operated in open-circuit for the period indicated by the dashed arrow between Fig. 6a and Fig. 6b. During this period, the MFCs reached a maximum open-circuit voltage of 789, 239, 316, and 561 mV, in the order of epoxy, PTFE, PVA, and PVDF, respectively. After performance

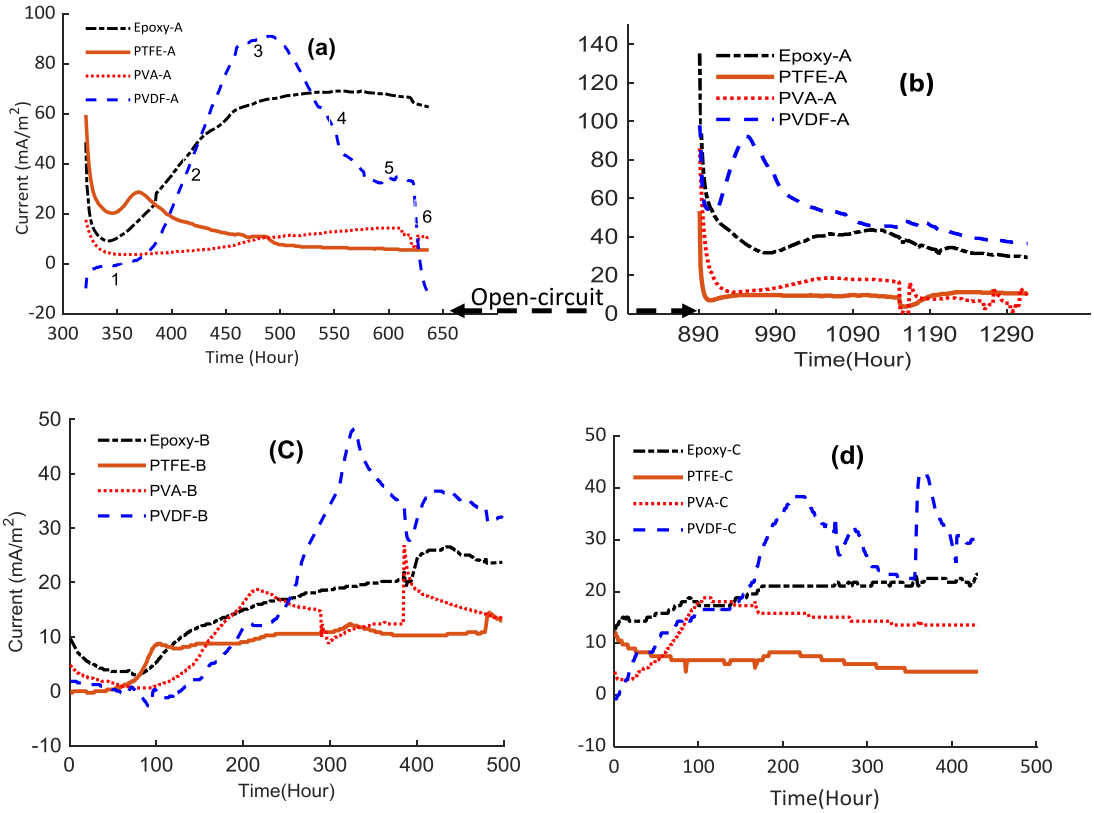

Fig. 6. performance of the binder at real-time external loads: (a) and (b) obtain from group A at an external load of 1kΩ, (c) and (d) from group B and Group C at 1kΩ and 470 Ω, respectivelyThe maximum specific growth rates of the cells were estimated by fitting the experimental data to the modified Gompertz model according to Equation 3.

determination through LSV at this point, the substrate was replenished and the load was reconnected to check the reproducibility of the binders' performance. The results of this second cycle of operation of the MFCs in group A are shown in Fig. 6b. Interestingly, PVDF reached approximately the same maximum current density in the first and second cycles (j= 91.32 and 92.224 mA/m^2 at V= 303 and 306 mV, respectively). This reproducible trend could indicate that the different binders favor the activities of certain bacteria. The drastic exponential drop in the current density of PVDF in the first cycle was no longer observed in the second cycle, as substrate was frequently replenished in all the MFCs once a decrease in performance was observed in PVDF. Epoxy also showed a similar performance trend as in the first cycle, but could not reach the same maximum current due to frequent treatment with SW. It is clear that the substrate needed to be replenished only when stable performance was achieved and a slight drop in performance was observed. However, in this study, the MFCs were treated in the same way to minimize the effects of experimental treatment bias. The same performance trend was observed in groups B and C, but with PVA producing higher current than PTFE. All MFCs achieved the best performance with a resistance of 1 kΩ compared to 470 Ω, while connecting the external load in the exponential growth phase and at maximum stable OCV resulted in better performance for the binders, except for PVDF, which initially had no noticeable change until the external load was connected. PVDF and epoxy showed better performance due to faster electron transfer at the electrodes, as shown by the low R_{ct} (Fig. 5). While the electrochemical performance using LSV showed that epoxy exhibited the best performance, which was sustained throughout the study period, PVDF generated a higher current at the two external loads tested. However, epoxy generated a more sustained current. Maintaining stable performance is critical to the application of MFCs, and therefore maximum performance should be maintained and not drop rapidly over relatively short periods [36], as demonstrated by the other binders used in this study. However, these binders could function differently when used independently as anode or cathode. This was not tested here, however, as the focus of the PR fabrication process is on producing highly conductive electrodes that can act as an anode and a cathode in an SMFC.

4. Conclusion

We tested the suitability of four different polymer binders (epoxy, PTFE, PVA, and PVDF) for the simple construction of a surface-modified stainless-steel (SS) electrode used as both anode and cathode in a soil microbial fuel cell for the generation of sustainable bioelectricity. PVDF generated the highest current of 92.2 mA/m^2 during long-term operation with an external load of 1 kΩ compared to epoxy, PTFE, and PVA, which generated 69.3, 28.9, and 14.5 mA/m^2, respectively. PTFE exhibited the fastest start-up behavior but deteriorated with time. Although epoxy did not produce the highest performance at the two external loads tested in this study, it showed more stable performance at the loads and the highest electrochemical performance during polarization, thus proving to be a suitable binder for easy fabrication of carbon black-modified SS electrodes for enhanced biopower generation from a SMFC. The deformation and resulting low performance of PVA over the operating time was attributed to the low degree of hydrolysis of the PVA used in this study. Therefore, further experiments with PVA with higher degree of hydrolysis are required to determine its suitability as an electrode in a SMFC.

Declaration of Competng Interest

The authors declare that they have no known competing financial interests or personal relationships that could have appeared to influence the work reported in this paper.

ACKNOWLEDGEMENTS

This study was supported by the Petroleum Technology Development Fund (PTDF), Nigeria, the German Academic Exchange Service (DAAD), and the Chair of Process Biotechnology, University of Bayreuth, Germany.

Supplementary materials

Supplementary material associated with this article can be found, in the online version, at doi:10.1016/j.ceja.2022.100246.

References

[1] X. Zhang, K. Guo, D. Shen, H. Feng, M. Wang, Y. Zhou, Y. Jia, Y. Liang, M. Zhou, Carbon black as an alternative cathode material for electrical energy recovery and transfer in a microbial battery, Sci. Rep. 7 (2017) 6981, 10.1038/s41598-017-07174-z.
[2] A. Baudler, I. Schmidt, M. Langner, A. Greiner, U. Schröder, Does it have to be carbon? metal anodes in microbial fuel cells and related bioelectrochemical systems, Energy Environ. Sci. 8 (2015) 2048–2055, https://doi.org/10.1039/C5EE00866B.
[3] S. Chen, S.A. Patil, R.K. Brown, U. Schröder, Strategies for optimizing the power output of microbial fuel cells: transitioning from fundamental studies to practical implementation, Appl. Energy (2019) 15–28, 233-23410.1016/j.apenergy.2018.10.015.
[4] J. Shanthi Sravan, A. Tharak, J.Annie Modestra, Seop Chang, S.Venkata Mohan, Emerging trends in microbial fuel cell diversification-Critical analysis, Bioresour. Technol. 326 (2021), 124676. 10.1016/j.biortech.2021.124676.
[5] H. Dong, H. Yu, X. Wang, Catalysis kinetics and porous analysis of rolling activated carbon-PTFE air-cathode in microbial fuel cells, Environ. Sci. Technol. 46 (2012), 13009–13015. 10.1021/es303619a.
[6] H. Dong, H. Yu, X. Wang, Q. Zhou, J. Feng, A novel structure of scalable air-cathode without Nafion and Pt by rolling activated carbon and PTFE as catalyst layer in microbial fuel cells, Water Res. 46 (2012) 5777–5787, https://doi.org/10.1016/j.watres.2012.08.005.
[7] B. Wei, J.C. Tokash, G. Chen, M.A. Hickner, B.E. Logan, Development and evaluation of carbon and binder loading in low-cost activated carbon cathodes for air-cathode microbial fuel cells, RSC Adv. 2 (2012) 12751–12758, https://doi.org/10.1039/C2RA21572A.
[8] F. Zhang, S. Cheng, D. Pant, G. van Bogaert, B.E. Logan, Power generation using an activated carbon and metal mesh cathode in a microbial fuel cell, Electrochem. Commun. 11 (2009) 2177–2179, https://doi.org/10.1016/j.elecom.2009.09.024.
[9] S. Cheng, H. Liu, B.E. Logan, Power densities using different cathode catalysts (Pt and CoTMPP) and polymer binders (Nafion and PTFE) in single chamber microbial fuel cells, Environ. Sci. Technol. 40 (2006) 364–369, https://doi.org/10.1021/es0512071.
[10] D. Pant, G. van Bogaert, M. de Smet, L. Diels, K. Vanbroekhoven, Use of novel permeable membrane and air cathodes in acetate microbial fuel cells, Electrochim. Acta 55 (2010) 7710–7716, https://doi.org/10.1016/j.electacta.2009.11.086.
[11] Z. Wang, G.D. Mahadevan, Y. Wu, F. Zhao, Progress of air-breathing cathode in microbial fuel cells, J. Power Sources 356 (2017) 245–255, https://doi.org/10.1016/j.jpowsour.2017.02.004.
[12] X.A. Walter, J. Greenman, I. Ieropoulos, Binder materials for the cathodes applied to self-stratifying membraneless microbial fuel cell, Bioelectrochemistry 123 (2018) 119–124, https://doi.org/10.1016/j.bioelechem.2018.04.011.
[13] X.A. Walter, C. Santoro, J. Greenman, I. Ieropoulos, Self-stratifying microbial fuel cell: the importance of the cathode electrode immersion height, Int. J. Hydrogen Energy 44 (2019) 4524–4532, https://doi.org/10.1016/j.ijhydene.2018.07.033.
[14] X.F. Chen, X.S. Wang, K.T. Liao, L.Z. Zeng, L.D. Xing, X.W. Zhou, X.W. Zheng, W. S. Li, Improved power output by incorporating polyvinyl alcohol into the anode of a microbial fuel cell, J. Mater. Chem. A 3 (2015) 19402–19409, https://doi.org/10.1039/C5TA03318G.
[15] N. Zafar, M.B.K. Niazi, F. Sher, U. Khalid, Z. Jahan, G.A. Shah, M. Zia, Starch and polyvinyl alcohol encapsulated biodegradable nanocomposites for environment friendly slow release of urea fertilizer, Chem. Eng. J. Adv. 7 (2021), 100123. 10.1016/j.ceja.2021.100123.
[16] S. Narayanasamy, J. Jayaprakash, Application of carbon-polymer based composite electrodes for Microbial fuel cells, Rev. Environ. Sci. Biotechnol. 19 (2020) 595–620, 10.1007/s11157-020-09545-x.
[17] A. Deeke, T.H.J.A. Sleutels, H.V.M. Hamelers, C.J.N. Buisman, Capacitive bioanodes enable renewable energy storage in microbial fuel cells, Environ. Sci. Technol. 46 (2012) 3554–3560, 10.1021/es204126r.
[18] W. Yang, W. He, F. Zhang, M.A. Hickner, B.E. Logan, Single-step fabrication using a phase inversion method of poly(vinylidene fluoride) (PVDF) activated carbon air cathodes for microbial fuel cells, Environ. Sci. Technol. Lett. 1 (2014) 416–420, 10.1021/ez5002769.
[19] N.'D.J. Koffi, S. Okabe, Domestic wastewater treatment and energy harvesting by serpentine up-flow MFCs equipped with PVDF-based activated carbon air-cathodes and a low voltage booster, Chem. Eng. J. 380 (2020), 122443. 10.1016/j.cej.2019.122443.

[20] M.I. Simeon, A.L. Imoize, R. Freitag, Comparative evaluation of the performance of a capacitive and a non-capacitive microbial fuel cell, in: 18th International Multi-Conference on Systems, Signals & Devices (SSD), IEEE, Monastir, Tunisia, 2021, 3/22/2021 - 3/25/2021, pp. 1076–1082. 10.1109/SSD52085.2021.9429481.
[21] M.I. Simeon, R. Freitag, Influence of electrode spacing and fed-batch operation on the maximum performance trend of a soil microbial fuel cell, Int. J. Hydrogen Energy (2021), https://doi.org/10.1016/j.ijhydene.2021.11.110.
[22] S. Wang, A. Adekunle, B. Tartakovsky, V. Raghavan, Synthesizing developments in the usage of solid organic matter in microbial fuel cells: a review, Chem. Eng. J. Adv. 8 (2021), 100140, 10.1016/j.ceja.2021.100140.
[23] I. Simeon, O.A. Raji, A. Gbabo, C. Okoro-Shekwaga, Performance of a single chamber soil microbial fuel cell at varied external resistances for electric power generation, J. Renew. Energy Environ. 3 (2016), https://doi.org/10.30501/jree.2016.70092.
[24] M.I. Simeon, F.U. Asoiro, M. Aliyu, O.A. Raji, R. Freitag, Polarization and power density trends of a soil-based microbial fuel cell treated with human urine, Int. J. Energy Res. 44 (2020) 5968–5976, https://doi.org/10.1002/er.5391.
[25] S.J. Dunaj, J.J. Vallino, M.E. Hines, M. Gay, C. Kobyljanec, J.N. Rooney-Varga, Relationships between soil organic matter, nutrients, bacterial community structure, and the performance of microbial fuel cells, Environ. Sci. Technol. 46 (2012) 1914–1922, 10.1021/es2032532.
[26] Y.-.B. Jiang, W.-.H. Zhong, C. Han, H. Deng, Characterization of electricity generated by soil in microbial fuel cells and the isolation of soil source exoelectrogenic bacteria, Front. Microbiol. 7 (2016) 1776, 10.3389/fmicb.2016.01776.
[27] S.Z. Abbas, M. Rafatullah, Recent advances in soil microbial fuel cells for soil contaminants remediation, Chemosphere 272 (2021), 129691. 10.1016/j.chemosphere.2021.129691.
[28] K. Herkendell, Status update on bioelectrochemical systems: prospects for carbon electrode design and scale-up, catalysts 11 (2021) 278. 10.3390/catal11020278.
[29] F. Zhao, R.C.T. Slade, J.R. Varcoe, Techniques for the study and development of microbial fuel cells: an electrochemical perspective, Chem. Soc. Rev. 38 (2009) 1926–1939, 10.1039/b819866g.
[30] J. Dziegielowski, B. Metcalfe, P. Villegas-Guzman, C.A. Martínez-Huitle, A. Gorayeb, J. Wenk, M. Di Lorenzo, Development of a functional stack of soil microbial fuel cells to power a water treatment reactor: from the lab to field trials in North East Brazil, Appl. Energy 278 (2020), 115680, 10.1016/j.apenergy.2020.115680.
[31] B. Yu, L. Feng, Y. He, L. Yang, Y. Xun, Effects of anode materials on the performance and anode microbial community of soil microbial fuel cell, J. Hazard. Mater. 401 (2021), 123394. 10.1016/j.jhazmat.2020.123394.
[32] H. Wang, S.Y. Sayed, E.J. Luber, B.C. Olsen, S.M. Shirurkar, S. Venkatakrishnan, U. M. Tefashe, A.K. Farquhar, E.S. Smotkin, R.L. McCreery, J.M. Buriak, Redox flow batteries: how to determine electrochemical kinetic parameters, ACS Nano 14 (2020) 2575–2584, https://doi.org/10.1021/acsnano.0c01281.
[33] A. Lasia, Electrochemical Impedance Spectroscopy and Its Applications, Springer, New York, New York, NY, 2014.
[34] T.S. Gaaz, A.B. Sulong, M.N. Akhtar, A.A.H. Kadhum, A.B. Mohamad, A.A. Al-Amiery, Properties and applications of polyvinyl alcohol, halloysite nanotubes and their nanocomposites, Molecules 20 (2015) 22833–22847.
[35] S.M. Martinez, M. Di Lorenzo, Electricity generation from untreated fresh digestate with a cost-effective array of floating microbial fuel cells, Chem. Eng. Sci. 198 (2019) 108–116, https://doi.org/10.1016/j.ces.2018.12.039.
[36] R. Rossi, B.E. Logan, Using an anion exchange membrane for effective hydroxide ion transport enables high power densities in microbial fuel cells, Chem. Eng. J. 422 (2021), 130150. 10.1016/j.cej.2021.130150. 10.1109/SSD52085.2021.9429481.